INTERNATIONAL JOURNAL OF INTEGRATED ENGINEERING
ISSN: 2229-838X e-ISSN: 2600-7916

IJIE

Vol. 16 No. 6 (2024) 216-227
https://publisher.uthm.edu.my/ojs/index.php/ijie

A Sensitivity Study of the Mathematical Model for Carbon Dioxide Removal by Physical Absorption in the Production of Biomethane from Palm Empty Fruit Bunch

Mohamad Afiq Mohd Asrul[1], Hafizah Abdul Halim Yun[1,2]*, Mohd Farid Atan[1,3,4,5], Ivy Ai Wei Tan[1], Josephine Chang Hui Lai[1,3]

[1] *Department of Chemical Engineering and Energy Sustainability, Faculty of Engineering, Universiti Malaysia Sarawak, Kota Samarahan, 94300, MALAYSIA*
[2] *Centre for Applied Learning and Multimedia (CALM), Universiti Malaysia Sarawak, Kota Samarahan, 94300, MALAYSIA*
[3] *Institute of Sustainable and Renewable Energy (ISURE), Universiti Malaysia Sarawak, Kota Samarahan, 94300, MALAYSIA*
[4] *Institute of Social Informatics and Technological Innovations (ISITI), Universiti Malaysia Sarawak, Kota Samarahan, 94300, MALAYSIA*
[5] *University Sustainable Centre (USC), Universiti Malaysia Sarawak, Kota Samarahan, 94300, MALAYSIA*

*Corresponding Author: ahyhafizah@unimas.my
DOI: https://doi.org/10.30880/ijie.2024.16.06.021

Article Info

Received: 12 August 2024
Accepted: 9 October2024
Available online: 5 November 2024

Keywords

Carbon dioxide capture, physical absorption, two-film theory, sensitivity analysis, mathematical model

Abstract

A non-equilibrium rate-based absorption model based on the two-film theory was adapted for the physical solvent in a packed bed column with co-counter current flow in place of chemical reaction. Carbon dioxide (CO_2) removal from fresh biomethane in a palm empty fruit bunch thermochemical conversion plant to improve the purity of the dried gas was modeled from the approximation of mathematical equations. This objective was achieved by improvising and reducing the model assumptions with guaranteed accuracy based on the validation using the established measured data. A better mathematical model with the predicted temperature profile at the liquid side and a mean absolute percentage error of less than 25% contributed to the 2 wt.% differences between the assumed dimethyl ether polyethylene glycol purity and the experiment, which is sufficient to be considered acceptable. To understand the performance of the absorption column, the sensitivity of three input variables on the removal of CO_2 was analyzed, including the temperature, pressure, and solvent feed flow rate by manipulating the input value for each variable individually. The optimum temperature of 31 °C, pressure of 1.6 kPa, and solvent feed flow rate of 1:1 liquid-to-gas ratio were established as the baseline values for the sensitivity test. The analysis from the mathematical model indicates a significant influence of the operating temperature on CO_2 absorption. This study enhances biomethane purity, optimizes CO_2 removal, and improves operational efficiency. It aligns with sustainability goals, reduces emissions, and offers economic benefits, making it valuable for the renewable energy industry.

1. Introduction

A two-film theory rate-based model has been extensively discussed in the gas purification study of carbon dioxide (CO_2) through chemical absorption. Nevertheless, little emphasis has been given to the analysis of the non-equilibrium (NEQ) characteristics of certain variables of interest using physical solvents. In the absence of chemical reactions, the capture of CO_2 by physical absorbents appears favorable under high-pressure and low-temperature operating conditions because its efficiency is directly related to Henry's law [1]. Challenges are expected to prove the possibility of the existing model to be compatible in the context of physical absorption. This is done by adjusting assumptions to ensure that ultimately, the error is within the acceptable range.

Gaspar et al. [2] applied a dynamic model of CO_2 chemical absorption with a simplified rigorous-based mass transfer model to numerically compute the efficiency of CO_2 capture at the gas stream outlet through the CO_2 concentration profile by varying the flow rates of flue gas. Gaspar and Cormos [3] evaluated a combined dynamic model of mass conservation and hydraulic correlation to optimally minimize the packing column dimension based on the sensitivity of the liquid-to-gas ratio (L:G) to the absorption rate, and four different classes of alkanolamine solution were compared. Similar to the SRP II model implemented by Tan et al. [4], the mass transfer of CO_2 from the gas phase to the liquid phase in steady-state counter-current CO_2 absorption by an inert absorbent to methane along a packed bed column was predicted at the elevated operating pressure of 0.1–5.0 MPa. Jayarathna et al. [5] revealed the high dependency of absorption rate, contact time, and phase equilibrium on the CO_2 removal efficiency, the CO_2 absorption heat as the driving force for the temperature gradient, and the influence of CO_2 absorbed availability to the rich loading rate using the NEQ rate-based model with the collaboration of Kent-Eisenberg model.

The difficulty in accomplishing the ideal equilibrium of CO_2 absorption has led to the rate-based model being the best option to date for the analysis of the real-time behavior of CO_2 separation. The rate-based NEQ model based on the two-film theory proposed by Pandya [6] was revised by Gabrielsen et al. [7] to describe the behavior changes of CO_2 and water vapor in a counter-current packed bed column with a uniform concentration and temperature at both the bulk side and the interphase, a considerable ideal binary mixture of vapor-liquid phase, and negligible solvent volatility and heat released to the surrounding. Based on the assumptions, Isa et al. [8] adapted Pandya's approach for the high CO_2 concentration in an adiabatic absorption tower operated at atmospheric pressure. The modification of Pandya's model was reported by Shahid et al. [9] with the exclusion of water vapor loss from the solvent in analyzing the CO_2 mass transfer behavior across two absorption regimes in a packed bed column. Shahid et al. [10] investigated the absorption rate as a function of CO_2 loading, which leads to the partitioning of the packed column into fast and slow regimes. This analysis considered high pressures up to 40 bar and high CO_2 concentrations in the evaluation of CO_2 removal efficiency, taking into account factors of liquid flow rates, solvent concentration, and CO_2 feed concentrations in the absence of axial dispersion, gas-liquid equilibrium according to the Peng-Robinson equation of state, and equivalent mass and heat transfer area.

In contrast to the previous studies, Shahid et al. [11] considered axial dispersion with an assumed fast gas-liquid separation rate in the liquid film and equilibrium in the liquid bulk when modeling a precisely structured packed column through a correlation analysis with mass transfer efficiency and effective mass transfer area for adiabatic CO_2 absorption at high liquid flow rates. Pakzad et al. [12] incorporated heat transfer at the liquid-gas interface based on the Chilton-Colburn analogy in the existing model to investigate the importance of the enhancement factor and mass transfer correlations for CO_2 absorption performance. Several key parameters were involved, such as the CO_2 composition in the liquid and gas phases, the temperature profile representing the heat release along the packing height, the solvent concentration relative to the CO_2 loading along the packing height, and the water distribution within the packing column as a function of temperature.

Regarding the gap in knowledge contribution, the two-film theory has been adapted for the rate-based mathematical model of CO_2 removal through physical absorption. The objective of the modeling study is to improve the purity of methane in dried gas as the product of the thermochemical conversion of palm empty fruit bunch (PEFB) through combined pyrolysis and direct methanation. To achieve the corresponding objective, the assumptions of the model are slightly refined with the validation against the real data retrieved from the studies of Kelly et al. [13] and Dave et al. [14]. The developed model is utilized in the sensitivity simulation to observe the influence of temperature, pressure, and feed flow rate on the removal of CO_2 from biomethane.

2. Mathematical Model: List of Assumptions

The rate-based model, derived from the two-film theory, was refined with minor adjustments to the assumptions to develop a mathematical model that can describe the physical absorption of CO_2 from biomethane as follows:

i. Equations (1)–(6): Mass and energy balances of a counter-current absorption model [9] for a packed bed column (Figure 1).

ii. Equation (7): The physical solvent used (i.e., dimethyl ether polyethylene glycol (DEPG)) that is inert to most gases, including water vapor [9], except CO_2 due to the higher solubility of water than CO_2 in DEPG [15].
iii. Equations (8) and (9): A vapor-liquid equilibrium model consists of the initial partial pressure of CO_2 at the interface.
iv. Equation (9): Henry's law constant of CO_2-DEPG [16].
v. Equations (10) and (11): Mass transfer of CO_2 in the liquid and gas phases, respectively [17].
vi. Equation (12): The wetted area of packing is assumed to be equal to the gas-liquid interfacial area [17].
vii. Equations (13)–(16): The presence of the side effect of CO_2 mass transfer in the liquid phase [18].

$$\frac{dF_G}{dz} = N_{CO_2} A_{eff} A_{column} \tag{1}$$

$$\frac{dy_{CO_2}}{dz} = \frac{N_{CO_2} A_{eff} A_{column} (y_{CO_2} - 1)}{F_G} \tag{2}$$

$$\frac{dF_L}{dz} = -N_{CO_2} A_{eff} A_{column} \tag{3}$$

$$\frac{dx_{CO_2}}{dz} = \frac{N_{CO_2} A_{eff} A_{column} (x_{CO_2} - 1)}{F_L} \tag{4}$$

$$\frac{dT_G}{dz} = \frac{q_{abs} A_{eff} A_{column}}{F_G cp_G} \tag{5}$$

$$\frac{dT_L}{dz} = \frac{N_{CO_2} cp_{CO_2} A_{eff} A_{column} (T_L - T_G)}{F_L cp_L} - \frac{q A_{eff} A_{column}}{F_L cp_L} + \frac{N_{CO_2} \Delta H_{abs}}{F_L cp_L} \tag{6}$$

$$N_{CO_2} = \frac{He_{CO_2} EP_{total} (y_{CO_2} - y_{CO_2,int})}{\frac{1}{k_{G,CO_2}} + \frac{He_{CO_2}}{E k_{L,CO_2}}} \tag{7}$$

$$p_{CO_2,i} = \frac{p_{CO_2}}{1 + \frac{E k_{L,CO_2}}{k_{G,CO_2}} He_{CO_2}} \tag{8}$$

$$He_{CO_2} = exp\left(13.828 - \frac{1720.0}{T}\right) \tag{9}$$

$$k_{G,CO_2} = 5.23 \left(\frac{F_G}{A_T \mu_{G,CO_2}}\right)^{0.7} \left(\frac{D_{G,CO_2-air} A_{td}}{RT}\right) \left(\frac{\mu_{G,CO_2}}{\rho_{G,CO_2} D_{G,CO_2-air}}\right)^{0.33} \left(A_{td} d_{packing}\right)^{-2.0} \tag{10}$$

$$k_{L,CO_2} = \frac{0.0051 \left(\frac{F_L}{A_{eff} \mu_{L,CO_2}}\right)^{0.67} \left(A_{td} d_{packing}\right)^{0.4}}{\left(\frac{\mu_{L,CO_2}}{\rho_{L,CO_2} D_{L,CO_2-DEPG}}\right)^{0.5} \left(\frac{\rho_{L,CO_2}}{\mu_{L,CO_2} g}\right)^{0.33}} \tag{11}$$

$$\frac{A_{eff}}{A_{td}} = 1 - exp\left[\begin{array}{l} -1.45 \left(\frac{\sigma_{critical,CO_2}}{\sigma_{L,CO_2}}\right)^{\frac{3}{4}} \left(\frac{F_L}{A_{td} \mu_{L,CO_2}}\right)^{0.1} \\ \times \left(\frac{{F_L}^2 A_T}{{\rho_{G,CO_2}}^2 g}\right)^{-\frac{1}{2}} \left(\frac{{F_L}^2}{\rho_{L,CO_2} \sigma_{L,CO_2} A_{td}}\right)^{0.2} \end{array}\right] \tag{12}$$

$$E = \frac{\sqrt{\frac{k_{CO_2-DEPG,2} D_{L,CO_2-DEPG} c_{0,DEPG}}{{k_{L,CO_2}}^2} (E_1 - E_0)}}{(E_1 - 1)}}{tan\left(\sqrt{\frac{k_{CO_2-DEPG,2} D_{L,CO_2-DEPG} c_{0,DEPG}}{{k_{L,CO_2}}^2} (E_1 - E_0)}}{(E_1 - 1)}\right)} \tag{13}$$

$$E_1 = 1 + \frac{D_{L,CO_2-DEPG} c_{0,DEPG}}{2 D_{L,CO_2-DEPG} c_{0,CO_2,i}} \tag{14}$$

$$E_0 = \sqrt{\frac{k_{CO_2-DEPG,2} D_{L,CO_2-DEPG} c_{0,DEPG}}{{k_{L,CO_2}}^2}} \tag{15}$$

$$k_{CO_2-DEPG,2} = 1.943 \times 10^7 exp\left(-\frac{5176.49}{T}\right) \tag{16}$$

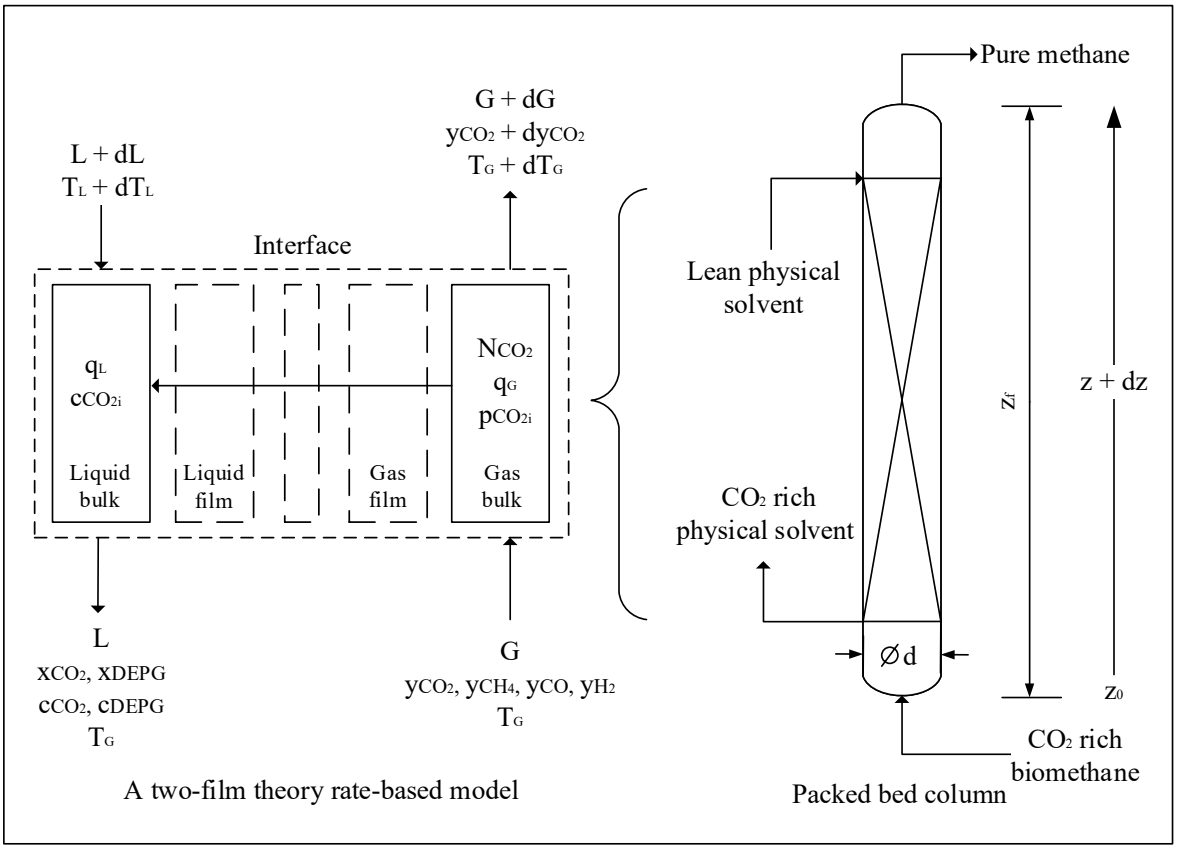

Fig. 1 *Illustration of a CO2 absorption model, an improvised version of Pandya [6], Gabrielsen et al. [7], and Shahid et al. [9]*

2.1 Implementation and Validation

The model was coded and executed using an ordinary differential equation (ODE) solver in MATLAB (R2019b, software license number: 40774331). The initial value for each input variable in the ODEs, as presented in Table 1, was based on the simulation data of raw biogas from the outlet of a steady-state IRMA isothermal reactor [19]. The constants and the mechanical design parameters, as listed in Table 2, were introduced to define the main equations. The results were then validated by calculating the determination of coefficient (R^2), mean absolute percentage error (MAPE), and mean square error (MSE) using Equations (17), (18), and (19), respectively. Both datasets were first normalized using Equation (20), which was based on the experimental runs by Kelly et al. [13]. The prediction from the model was made once the resulting error was lower than those reported in the literature.

2.2 Sensitivity Analysis

The confirmed mathematical model was utilized in the sensitivity study to observe the degree of influence for each input variable (temperature, pressure, and feed flow rate) on the response of CO_2 removal. The sensitivity test was conducted according to a profile method, where the base value of one variable was manipulated gradually at a time, with change ratios of 25%, 50%, and 75%, while the remaining variables were kept constant.

3. Results and Discussion

A mathematical model of CO_2 physical absorption from biomethane was developed, and the least error of approximation (temperature profile of the liquid and gas streams) was identified using the ODE45 solver by adjusting the design parameters according to literature values [20], as presented in Table 3, after several iterations of trial-and-error. The significant selective CO_2 removal by the co-counter current flow absorption can be seen toward the end of the column distance, as illustrated in Figure 2. Moving from downstream to upstream, the CO_2 content in biogas decreased by up to 95% from its initial concentration, while the CO_2 content in DEPG exhibited an opposite trend due to the dissolving of CO_2.

Int. Journal of Integrated Engineering Vol. 16 No. 6 (2024) 216-227

Table 1 *Main characteristics of biomethane feedstock data* [19]

Operating condition	Value
Methanator temperature (°C)	26.8
Methanator pressure (kPa)	2700
Flow rate of the outlet gas stream of the gasifier (kmol/s)	0.0131
Dry gas composition (mol%)	
CH_4	52.5
CO_2	45.1
CO	0.0
H_2	2.4

Table 2 *Design data of a structured packing column of CO_2 absorber* [20]

Design parameter	Value / detail	Unit
Column diameter	28.0	mm
Total height of column	2.16	m
Material construction	Stainless steel	
Packing model	Structured Sulzer DX	
Interfacial area/wet surface area per unit packing volume	900	m^2/m^3
Packing length	0.054	m
Packing number	40	

$$R^2 = 1 - \frac{\sum(Predicted\ data - Measured\ data)^2}{\sum(Measured\ data - Mean\ of\ measured\ data)^2} \quad (17)$$

$$MSE = \frac{\sum(measured\ data - predicted\ data)^2}{number\ of\ data} \quad (18)$$

$$MAPE\ (\%) = \frac{\sum \frac{|measured\ data - predicted\ data| \times 100\ \%}{measured\ data}}{number\ of\ data} \quad (19)$$

$$Normalised\ data = \frac{0.8(Scale\ data\ point - minimum\ data\ point)}{(maximum\ data\ point - minimum\ data\ point)} + 0.1 \quad (20)$$

In the first quarter of the packed bed column from the upstream, the CO_2 absorbed was rapid due to the relatively lean feed solvent [21]. The pure DEPG promoted the expansion of CO_2 loading by at least 65% without fluctuations in CO_2 concentration due to the absence of water vapor in the biogas, which agreed with the model assumption (ii.). Then, it was noticeable that the concentration decreased progressively. This is because the occupied CO_2 had reached the maximum capacity of the solvent for optimum absorption, indicating that both gas and liquid phases of CO_2 are at an equilibrium state. The absorption rate slowed down near the downstream because the solvent was semi-contaminated with CO_2 impurity [21]. In addition, the low rate was attributed to the low residence of the packing column, where the gas-liquid phase contact surface area was largely dependent on the column diameter and type, as well as the height of the packing used [22].

It can be said that the reference correlations used to define the parameters in the main equations, including the physical properties of the solvent and the surface tension, must be compatible with the characteristics of the structured packing. This is because the packing significantly influences the overall efficiency of gas-liquid mass transfer in the packed bed column, as well as the operational key variables (i.e., total pressure of the absorber, concentration, and CO_2 loading rate of the DEPG solvent). The model's prediction of the given CO_2 concentration profile appeared to be specific for the initial composition of CO_2 in biomethane at 40.051 mol%.

3.1 Model Validation

The accuracy of the mathematical model was proven by the dual confirmation from qualitative and quantitative analyses. From Figure 3, the predicted liquid-side temperature was relatively close to the actual data, with a slight deviation that enhances process control and optimization. This improvement makes CO_2 absorption more economically feasible in terms of operational costs and energy consumption.

This is contributed by the correlations where the assumption is made to address that DEPG has 100% purity. In contrast to the material used in the reference experiment, DEPG consisted of 2 wt.% water that was intentionally added to overcome the mild conditions of the operating packed bed column for purifying high-pressure gases. The study shows that CO_2 capture remains effective even at 2 wt.% water content in DEPG, suggesting that extremely high solvent purity is not required, which can reduce costs and simplify handling and storage. The prediction showed good agreement with the measurement from the experiment conducted by Kelly

et al. [13], with the calculated R^2 = 0.972, MSE = 9.017 × 10^{-3}, and MAPE = 20.43%. Due to the physical absorption resulting from the in-contact co-counter current flow, the warm biogas from the downstream (z = 0.00 m) and the cold solvent of DEPG fed from the upstream (z = 2.16 m) simultaneously shifted their respective temperature until the net heat transfer was achieved. This explains the exponential temperature profile pattern in both side streams. The rate-based absorption model significantly improved the prediction error from 36.84% as reported by Kelly et al. [13] to as low as 20.43% for the characteristic study on the physical removal of CO_2 by DEPG. Therefore, the model assumptions were adequately validated and are scalable, providing insights into heat transfer mechanisms that can enhance the design and operation of biomethane gas cleaning on an industrial scale.

Table 3 *Final iteration input values of the mathematical model for CO_2 physical absorption*

Parameter	Symbol	Value	Unit
Packed bed column distance			
Initial	z_0	0.00	m
Final	z_f	2.16	m
Initial guess of ODE variables			
Feed flow rate of PEFB-derived biomethane	G	13.111	mol/s
CO_2 mole fraction in feed biomethane	yCO_2	0.4051	
Feed flow rate of DEPG physical solvent	L	13.111	mol/s
CO_2 mole fraction in feed DEPG physical solvent	xCO_2	0.0000	
Gas-side temperature	T_G	26.8	°C
Liquid-side temperature	T_L	25.0	°C
Mechanical design parameter of the absorber			
Total dry surface area of packing	A_t	900.0	m^2/m^3
Number of packings	n	36	
Column diameter	d	2.0	cm
Packing size	d_p	0.54	m
Operating conditions of CO_2 absorption			
Temperature	T	31.0	°C
Total pressure	P	162.12	kPa
Purity of DEPG solvent	x_{DEPG}	1.0	
Concentration of DEPG	C_{DEPG}	1.0	mol/m^3
Concentration of CO_2	CCO_2	2.0	mol/m^3

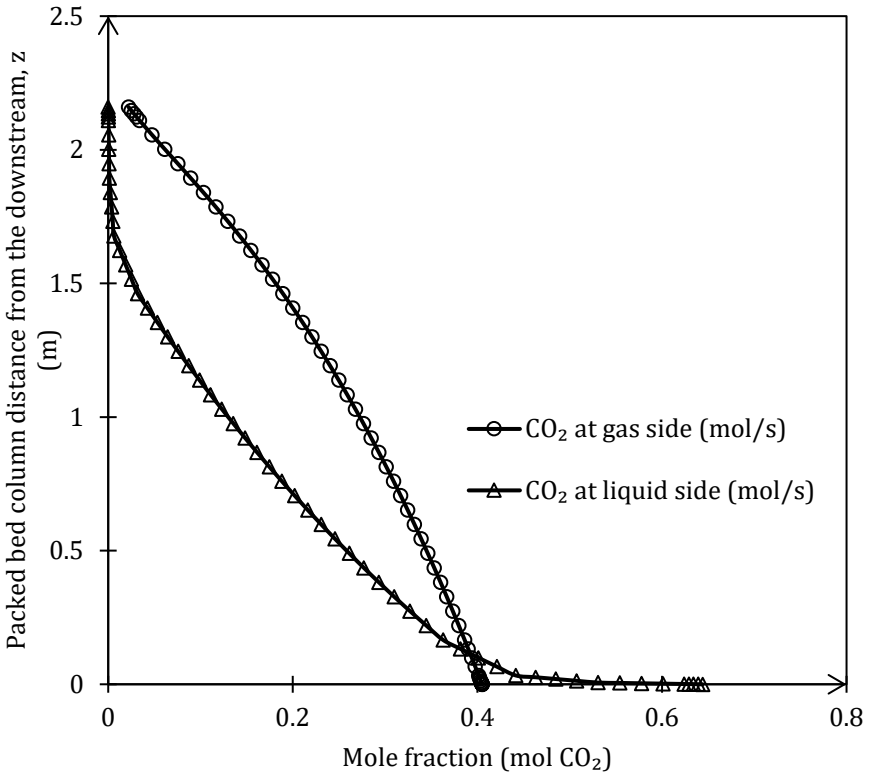

Fig. 2 *CO2 concentration profile along the packing column distance from the bottom*

Int. Journal of Integrated Engineering Vol. 16 No. 6 (2024) 216-227

However, the temperature profile overestimates the pilot data from a packed tower simulation work [14] with R^2 = 0.603, MSE = 0.168, and MAPE = 46.17%. This discrepancy indicates that the modelling assumptions have limitations as they do not always maintain the same operating conditions of the physical absorbent, including variations in water content, solvent feed temperature, and flow rates, which could affect CO_2 absorption efficiency and overall performance. Moreover, increasing the size of the packed bed column may introduce complexities that are not considered in the model, such as flow distribution and column dimensions.

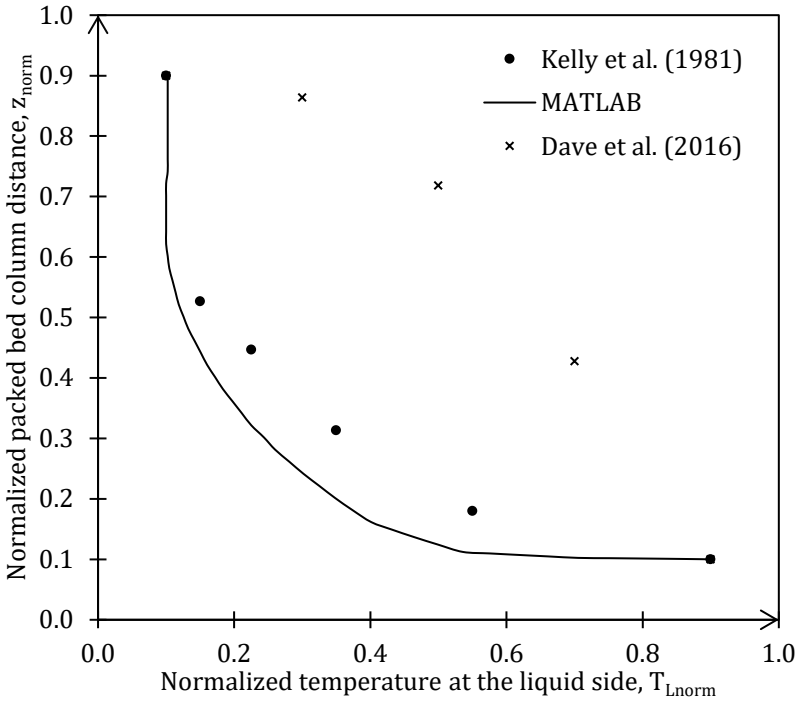

Fig. 3 *Predicted (MATLAB) versus experimental data [13,14] of the temperature profile at the liquid side*

3.2 Sensitivity Analysis

From the final iteration of the mathematical model, the optimum value of each input parameter was identified as T = 31 °C, P = 1.6 kPa, and L:G =1:1, which have been referred to as the benchmark in this sensitivity test. Figure 4 shows that operating temperature is the most sensitive input factor for CO_2 removal, as indicated by the significant difference in the minimum CO_2 concentration in the range of 0%–75% reduction from its base value. The efficiency of DEPG capacity to absorb CO_2 losses decreased outside the room temperature range, whether the condition is colder or slightly warmer. A stable operating temperature significantly improves the upgrading of biomethane gas with efficient absorption of CO_2, especially for industrial purposes. Therefore, the temperature of lean solvent needs to be monitored after regeneration through pressure flashing before it can be recycled to the upstream of the column, with adjustments made by heat exchangers or cooling systems to ensure that it remains within the optimum range. On the other hand, an increase in solvent temperature due to the co-counter current contact with the warm biogas could contribute to an increase in the absorbent's viscosity, which will reduce CO_2 solubility in DEPG [22]. This necessitates the installation of mechanisms to control and mitigate temperature increases, such as insulated columns or temperature-controlled environments. Maintaining a constant temperature of 31 °C in industrial environments can be challenging due to external environmental conditions and the heat generated during CO_2 absorption. Future research should investigate advanced cooling and heating systems that can dynamically adapt to temperature fluctuations and explore the use of novel solvents that are less sensitive to temperature fluctuations.

The second influential factor is the feed flow rate of liquid solvent, as indicated by the uniform gap of the minimum CO_2 concentration from 0% to a 75% increase from its benchmark point. The efficiency of CO_2 absorption increased with the narrowing gap of the feed flow rate between the biogas and DEPG. This observation is consistent with the findings of Kelly et al. [13], suggesting that a slightly low or equivalent L:G of the feed flow rate promotes a longer retention time of the co-counter current gaseous flow to the physical solvent in a packed bed column to achieve optimum CO_2 absorption. Regardless of flooding prevention, the liquid ratio should be equal to or lower than the gas feed flow rate [23]. Automated control systems and sensors should be provided in the packed bed column to allow precise adjustment of liquid and gas feed flow rates in real-time to maintain the optimum L:G and ensure sufficient retention time for gas-solvent interaction. Achieving and maintaining an exact

L:G of 1:1 can be difficult in large-scale plants due to variations in biomethane feed and operating conditions. Therefore, robust control algorithms and sensor technologies need to be developed to improve the precision of flow rate adjustments and investigate the effect of different L:G ratios on CO_2 absorption efficiency under different operating conditions.

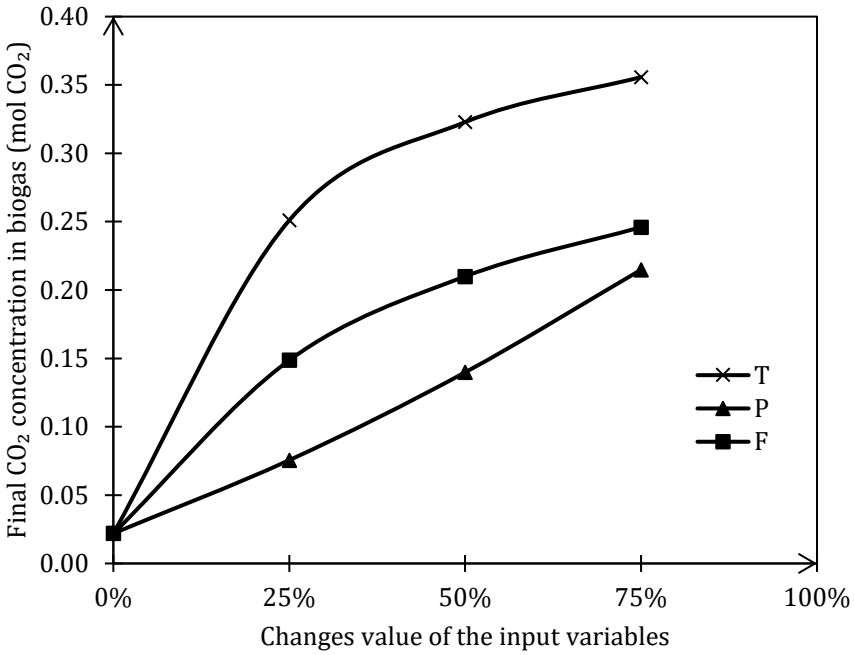

Ratio of the changes (%)	0	25	50	75
T (°C)	31.0	23.2	15.5	7.75
P (kPa)	1.6	1.2	0.8	0.4
F (L:G)	1:1	4:5	2:3	4:7

Fig. 4 *Sensitivity analysis based on the profile method*

Among the three input parameters, pressure was ranked the least sensitive to changes in CO_2 removal. CO_2 absorption efficiency increased with the gradual rise in operating pressure, as indicated by the consistent changes from 75% to 0%, which was limited until the atmospheric condition. The solubility of CO_2 in the physical solvent is expressed as a function of CO_2 partial pressure. The selection of packing design is also vital to maintain the optimum pressure drop for CO_2 transfer with respect to surface area uniformity and column size, resulting in the friction loss of CO_2 into DEPG during absorption [16]. This necessitates investment in high-quality packing materials and appropriate column design to minimize friction losses. Pressure fluctuations can still affect the overall efficiency and safety of the system. Therefore, pressure-resistant materials and column designs that can withstand higher pressures without compromising efficiency need to be explored, and the combined effects of pressure and other parameters on CO_2 absorption in different industrial environments need to be investigated.

Changes in solvent properties such as viscosity and solubility can affect CO_2 absorption efficiency, and the interaction between the solvent and the biogas components can introduce impurities that affect performance. Therefore, it is necessary to investigate the long-term stability and performance of DEPG and other physical solvents under different industrial conditions and to develop new solvents or solvent blends with improved thermal and chemical stability. The economic feasibility and environmental impact of maintaining optimum conditions for CO_2 absorption must be considered. This requires life-cycle analyses and cost-benefit analyses to determine the most sustainable and cost-effective methods for CO_2 capture and to investigate alternative energy sources and waste heat recovery systems to reduce operating costs and environmental impact.

4. Conclusions

The incorporation of CO_2-DEPG solvent correlations in a rate-based model based on the two-film theory has demonstrated the capability to estimate CO_2 removal from biomethane through physical absorption. The input data of the feed biogas were obtained from the thermochemical pilot plant model of PEFB conversion. The model was validated with a better MAPE of the temperature profile, as low as 20.43%. Using the profile method, the sensitivity analysis of the mathematical model revealed that the operating temperature has the most significant effect on CO_2 removal compared to the pressure of the packed bed column and the feed flow rate ratio of the liquid solvent to the biogas. Enhanced CO_2 removal efficiency contributes to the reduction of greenhouse gas emissions, aligning with environmental regulations and sustainability goals for a cleaner industrial process. Future research

should focus on validating real-world data through pilot-scale experiments to refine the model, incorporate advanced computational techniques and real-time monitoring for improved predictive capabilities, explore alternative solvents for more effective CO_2 removal, and investigate the long-term performance and stability of DEPG with different impurities for continuous operation and maintenance strategies.

Acknowledgement

The authors would like to thank the Department of Chemical Engineering and Energy Sustainability, Faculty of Engineering, Universiti Malaysia Sarawak for providing the research facilities to conduct this research. Finally, the authors would like to express gratitude to those who contributed directly or indirectly to the success of this research. This research did not receive any specific grant from funding agencies in the public, commercial, or not-for-profit sectors.

Conflict of Interest

Authors declare that there is no conflict of interests regarding the publication of the paper.

Author Contribution

The authors confirm contribution to the paper as follows: ***study conception and design:*** *Mohamad Afiq Mohd Asrul, Hafizah Abdul Halim Yun;* ***data collection:*** *Mohamad Afiq Mohd Asrul, Hafizah Abdul Halim Yun;* ***analysis and interpretation of results:*** *Mohamad Afiq Mohd Asrul, Hafizah Abdul Halim Yun;* ***draft manuscript preparation:*** *Mohamad Afiq Mohd Asrul, Hafizah Abdul Halim Yun, Mohd Farid Atan, Ivy Ai Wei Tan, Josephine Chang Hui Lai. All authors reviewed the results and approved the final version of the manuscript.*

Appendix A: Supplementary Information

Table A1 *List of physical property correlations required by the mathematical model*

Property	Correlations
Critical CO_2 surface tension in liquid interphase	$\boldsymbol{\sigma_C = \left(-0.951 + \frac{0.432}{Z_C}\right)(1 - T_r)^{\frac{11}{9}}(P_c^2 T_c)^{\frac{1}{3}}}$ Where, $Z_C = \frac{1}{R}\left(\frac{P_c V_c}{T_c}\right), \quad T_r = \frac{T}{T_c}$
CO_2 surface tension in liquid interphase	$\boldsymbol{\sigma_L = (1.201 \times 10^2 - 1.618 \times 10^{-1} T) + \left((1.443 \times 10^2 - 1.523T)x_{DEPG}\right) + \left((-2.287 \times 10^3 + 1.170 \times 10T)x_{DEPG}{}^2\right) + \left((6.716 \times 10^3 - 2.982 \times 10T)x_{DEPG}{}^3\right) + \left((-7.351 \times 10^3 + 3.078 \times 10T)x_{DEPG}{}^4\right) + \left((2.723 \times 10^3 - 1.109 \times 10T)x_{DEPG}{}^5\right)}$
CO_2 liquid-phase density	$\boldsymbol{\rho_L = 1030.59 - 9.25284 \times 10^{-1} T - 6.91297 \times 10^{-6} T^2}$
CO_2 gas-phase density	$\boldsymbol{\rho_G = -2.148 \times 10^5 + 1.168 \times 10^4 T - 2.302 \times 10^2 T^2 + 1.967 T^3 - 6.185 \times 10^{-3} T^4 + (4.757 \times 10^2 - 2.619 \times 10T + 5.215 \times 10^{-1} T^2 - 4.494 \times 10^{-3} T^3 + 1.423 \times 10^{-5} T^4)P + (-3.714 \times 10^{-1} + 2.072 \times 10^{-2} T - 4.169 \times 10^{-4} T^2 + 3.623 \times 10^{-6} T^3 - 1.155 \times 10^{-8} T^4)P^2 + (1.229 \times 10^{-4} - 6.93 \times 10^{-6} T + 1.406 \times 10^{-7} T^2 - 1.231 \times 10^{-9} T^3 + 3.948 \times 10^{-12} T^4)P^3 + (-1.466 \times 10^{-8} + 8.338 \times 10^{-10} T - 1.704 \times 10^{-11} - T^2 + 1.501 \times 10^{-13} T^3 - 4.839 \times 10^{-16} T^4)P^4}$
Liquid-phase viscosity	$\boldsymbol{\mu_L = \exp\left(-2.681 + \frac{8.103 \times 10^2}{T} - \frac{8.718 \times 10^3}{T^2}\right) + 5.518 \times 10^1 - \frac{3.559 \times 10^4}{T} + \frac{5.886 \times 10^6}{T^2} x_{DEPG} + \left(8.755 - \frac{8.704 \times 10^3}{T} + \frac{1.824 \times 10^6}{T^2} x_{DEPG}{}^2\right) + \left(-5.344 \times 10^2 + \frac{3.542 \times 10^5}{T} - \frac{5.810 \times 10^7}{T^2} x_{DEPG}{}^3\right) + 8.809 \times 10^2 - \frac{5.781 \times 10^5}{T} + \frac{9.385 \times 10^7}{T^2} x_{DEPG}{}^4 + \left(-4.080 \times 10^2 + \frac{2.669 \times 10^5}{T} - \frac{4.322 \times 10^7}{T^2} x_{DEPG}{}^5\right)}$
Gas-phase viscosity	$\boldsymbol{\mu_G = (-1.958 \times 10 + 1.123T - 2.32 \times 10^{-2} T^2 + 2.067 \times 10^{-4} T^3 - 6.74 \times 10^{-7} T^4) + (4.187 \times 10^{-2} - 2.426 \times 10^{-3} T + 5.051 \times 10^{-5} T^2 - 4.528 \times 10^{-7} T^3 + 1.484 \times 10^{-9} T^4)P + (-3.164 \times 10^{-5} + 1.853 \times 10^{-6} T - 3.892 \times 10^{-8} T^2 + 3.512 \times 10^{-10} T^3 - 1.157 \times 10^{-12} T^4)P^2 + (1.018 \times 10^{-8} - 6.014 \times 10^{-10} T - 1.272 \times 10^{-11} T^2 - 1.154 \times 10^{-13} T^3 - 3.819 \times 10^{-16} T^4)P^3 + (-1.186 \times 10^{-12} + 7.052 \times 10^{-14} T - 1.5 \times 10^{-15} T^2 + 1.368 \times 10^{-17} T^3 - 4.545 \times 10^{-20} T^4)P^4}$
Gas-phase diffusivity of CO_2-DEPG	$D_{CO_2-DEPG,G} = 2.35 \times 10^{-6}\, exp\left(-\frac{2119}{T}\right)$
Liquid phase diffusivity of CO_2-DEPG	$\boldsymbol{D_{CO_2-DEPG,L} = 9.89 \times 10^{-8}\, T \mu_{DEPG}{}^{-0.907} V_1{}^{-0.45} V_2{}^{0.265}}$
Molar volume of DEPG	$\boldsymbol{V_{DEPG} = 2.15688 \times 10^{-4} + 1.92822 \times 10^{-7} T + 1.98626 \times 10^{-10} T^2}$

Int. Journal of Integrated Engineering Vol. 16 No. 6 (2024) 216-227

Table A2 *Processed data 1 used in validating the mathematical model (the liquid-side temperature profile)*

Kelly et al. [13] (measured)		MATLAB (predicted)		Normalized data			$(T_{measured} - T_{predicted})^2$	$\lvert(T_{measured}-T_{predicted})\rvert \times 100\% / T_{measured}$
z (ft)	T_l (°F)	z (m)	T_l (K)	z	$T_{measured}$	$T_{predicted}$		
3.0	-5.0	2.16	298.15	0.90	0.10	0.10	0.000	0.00
1.6	-4.0	1.16	298.21	0.53	0.15	0.12	0.001	20.00
1.3	-2.5	0.95	298.34	0.45	0.23	0.15	0.006	35.56
0.8	0.0	0.57	298.72	0.31	0.35	0.23	0.014	34.29
0.3	4.0	0.22	299.32	0.18	0.55	0.37	0.032	32.73
0.0	11.0	0.00	301.49	0.10	0.90	0.90	0.000	0.00
					R^2 =	0.972		
					$MSE = \Sigma(T_{measured}-T_{predicted})^2/N$ =		9.017×10^{-3}	
					$MAPE = \Sigma(\lvert T_{measured}-T_{predicted}\rvert \times 100\ \%/T_{measured})/N$ =		20.43%	

Table A3 *Processed data 2 used in validating the mathematical model (the liquid-side temperature profile)*

Dave et al. [14] (measured)		MATLAB (predicted)		Normalized data			$(T_{measured} - T_{predicted})^2$	$\lvert(T_{measured}-T_{predicted})\rvert \times 100\% / T_{measured}$
z (m)	T_l (°C)	z (m)	T_l (K)	z	$T_{measured}$	$T_{predicted}$		
25	22.5	2.16	298.15	0.90	0.10	0.10	0.000	0.00
20	27.0	1.62	298.14	0.70	0.43	0.10	0.107	76.60
15	31.0	1.08	298.25	0.50	0.72	0.13	0.351	82.53
10	33.0	0.54	298.76	0.30	0.86	0.24	0.384	71.75
5	33.5	0.22	299.32	0.10	0.90	0.90	0.000	0.00
					R^2 =	0.603		
					$MSE = \Sigma(T_{measured}-T_{predicted})^2/N$ =		0.168	
					$MAPE = \Sigma(\lvert T_{measured}-T_{predicted}\rvert \times 100\ \%/T_{measured})/N$ =		46.17%	

Table A4 *The recorded data obtained from the sensitivity simulation of the mathematical model*

Changes ratio (%)	Feed flow rate of liquid solvent		Temperature		Pressure	
	L:G	yCO_2 (mol CO_2)	T (°C)	yCO_2 (mol CO_2)	P (kPa)	yCO_2 (mol CO_2)
Base	1:1	0.0220	31.0	0.0220	1.6	0.0220
25	4:5	0.1486	23.2	0.2510	1.2	0.0756
50	2:3	0.2100	15.5	0.3228	0.8	0.1398
75	4:7	0.2460	7.75	0.3558	0.4	0.2148

References

[1] Vega, F., Cano, M., Camino, S., Fernández, L. M. G., Portillo, E., & Navarrete, B. (2018). Solvents for Carbon Dioxide Capture. In *Carbon Dioxide Chemistry, Capture and Oil Recovery*. InTech. https://doi.org/10.5772/intechopen.71443

[2] Gaspar, J., Jorgensen, J. B., & Fosbol, P. L. (2015). A dynamic mathematical model for packed columns in carbon capture plants. *2015 European Control Conference (ECC)*, 2738–2743. https://doi.org/10.1109/ECC.2015.7330952

[3] Gaspar, J., & Cormos, A.-M. (2012). Dynamic modeling and absorption capacity assessment of CO2 capture process. *International Journal of Greenhouse Gas Control*, *8*, 45–55. https://doi.org/10.1016/j.ijggc.2012.01.016

[4] Tan, L. S., Shariff, A. M., Tay, W. H., Lau, K. K., & Halim, H. N. A. (2016). Integrated mathematical modeling for prediction of rich CO 2 absorption in structured packed column at elevated pressure conditions. *Journal of Natural Gas Science and Engineering*, *28*, 737–745. https://doi.org/10.1016/j.jngse.2015.11.004

[5] Jayarathna, S. A., Lie, B., & Melaaen, M. C. (2013). Dynamic modelling of the absorber of a post-combustion CO2 capture plant: Modelling and simulations. *Computers & Chemical Engineering*, *53*, 178–189. https://doi.org/10.1016/j.compchemeng.2013.03.002
[6] Pandya, J. D. (1983). Adiabatic gas absorption and stripping with chemical reaction in packed towers. *Chemical Engineering Communications*, *19*(4–6), 343–361. https://doi.org/10.1080/00986448308956351
[7] Gabrielsen, J., Michelsen, M. L., Stenby, E. H., & Kontogeorgis, G. M. (2006). Modeling of CO2 absorber using an AMP solution. *AIChE Journal*, *52*(10), 3443–3451. https://doi.org/10.1002/aic.10963
[8] Isa, F., Zabiri, H., Ramasamy, M., Tufa, L. D., Shariff, A. M., & Saleh, S. F. (2017). Pressure modification index based on hydrodynamics and mass transfer effects for modeling of CO 2 removal from natural gas via absorption at high pressures. *International Journal of Greenhouse Gas Control*, *56*, 173–186. https://doi.org/10.1016/j.ijggc.2016.11.024
[9] Shahid, M. Z., Maulud, A. S., Bustam, M. A., Suleman, H., Halim, H. N. A., & Shariff, A. M. (2019). Rate-based modeling for packed absorption column of the MEA–CO2 –water system at high-pressure and high-CO2 loading conditions. *Industrial & Engineering Chemistry Research*, *58*(27), 12235–12246. https://doi.org/10.1021/acs.iecr.9b01482
[10] Shahid, M. Z., Maulud, A. S., Bustam, M. A., Suleman, H., Abdul Halim, H. N., & Shariff, A. M. (2021). Packed column modelling and experimental evaluation for CO2 absorption using MDEA solution at high pressure and high CO2 concentrations. *Journal of Natural Gas Science and Engineering*, *88*, 103829. https://doi.org/10.1016/j.jngse.2021.103829
[11] Shahid, M. Z., Maulud, A. S., Azmi Bustam, M., & Suleman, H. (2020). Modeling of CO 2 -MEA absorption system in the packed column using Sulzer DX structured packing. *IOP Conference Series: Materials Science and Engineering*, *736*(2), 022059. https://doi.org/10.1088/1757-899X/736/2/022059
[12] Pakzad, P., Mofarahi, M., & Lee, C.-H. (2021). Sensitivity analysis of mass transfer and enhancement factor correlations for the absorption of CO2 in a Sulzer DX packed column using 4-diethylamino-2-butanol (DEAB) solution. *Separation and Purification Technology*, *268*, 118696. https://doi.org/10.1016/j.seppur.2021.118696
[13] Kelly, R. M., Rousseau, R. W., & Ferrell, J. K. (1981). Physical absorption of CO2 and sulfur gases from coal gasification: Simulation and experimental results. *Separation Science and Technology*, *16*(10), 1389–1414. https://doi.org/10.1080/01496398108058308
[14] Dave, A., Dave, M., Huang, Y., Rezvani, S., & Hewitt, N. (2016). Process design for CO2 absorption from syngas using physical solvent DMEPEG. *International Journal of Greenhouse Gas Control*, *49*, 436–448. https://doi.org/10.1016/j.ijggc.2016.03.015
[15] Rackley, S. A. (2017). Carbon capture from power generation. In *Carbon Capture and Storage* (pp. 75–101). Elsevier. https://doi.org/10.1016/B978-0-12-812041-5.00004-0
[16] Kapetaki, Z., Brandani, P., Brandani, S., & Ahn, H. (2015). Process simulation of a dual-stage Selexol process for 95% carbon capture efficiency at an integrated gasification combined cycle power plant. *International Journal of Greenhouse Gas Control*, *39*, 17–26. https://doi.org/10.1016/j.ijggc.2015.04.015
[17] Onda, K., Takeuchi, H., & Okumoto, Y. (1968). Mass transfer coefficients between gas and liquid phases in packed columns. *Journal of Chemical Engineering of Japan*, *1*(1), 56–62. https://doi.org/10.1252/jcej.1.56
[18] van Krevelen, D. W., & Hoftijzer, P. J. (1948). Kinetics of gas-liquid reactions part I. General theory. *Recueil Des Travaux Chimiques Des Pays-Bas*, *67*(7), 563–586. https://doi.org/10.1002/recl.19480670708
[19] Yun, H. A. H., Ramírez-Solís, S., & Dupont, V. (2020). Bio-CH4 from palm empty fruit bunch via pyrolysis-direct methanation: Full plant model and experiments with bio-oil surrogate. *Journal of Cleaner Production*, *244*, 118737. https://doi.org/10.1016/j.jclepro.2019.118737
[20] deMontigny, D., Aboudheir, A., Tontiwachwuthikul, P., & Chakma, A. (2006). Modelling the performance of a CO2 absorber containing structured packing. *Industrial & Engineering Chemistry Research*, *45*(8), 2594–2600. https://doi.org/10.1021/ie050567u
[21] Adams, T. A., Salkuyeh, Y. K., & Nease, J. (2014). Processes and simulations for solvent-based CO2 capture and syngas cleanup. In *Reactor and Process Design in Sustainable Energy Technology* (pp. 163–231). Elsevier. https://doi.org/10.1016/B978-0-444-59566-9.00006-5
[22] Sreedhar, I., Nahar, T., Venugopal, A., & Srinivas, B. (2017). Carbon capture by absorption – Path covered and ahead. *Renewable and Sustainable Energy Reviews*, *76*, 1080–1107. https://doi.org/10.1016/j.rser.2017.03.109
[23] Bell, D. A., Towler, B. F., & Fan, M. (2011). Sulfur Recovery. In *Coal Gasification and Its Applications* (pp. 113–136). Elsevier. https://doi.org/10.1016/B978-0-8155-2049-8.10006-3